The Fusion Driven Rocket

Nuclear Propulsion through Direct Conversion of Fusion Energy

**John Slough, Anthony Pancotti, George Votroubek, David Kirtley,
Christopher Pihl, Michael Pfaff**

MSNW LLC
8551 154th Avenue NE, Redmond WA 98052
sloughj@msnwllc.com

Challenges associated with deep space travel

Long Trip Times

- Radiation exposure Cancer risk
- Mental fatigue
- Increased risk of critical failure
- Bone & muscle loss
- Public interest
- Governmental support

High Costs

- Operational costs
- Complexity Pre-deployed assets Space assembly
- Huge fuel Mass
- Large space structures

Conclusion:
Manned space exploration faces many safety, political, direct cost, and launch costs

New method of propulsion is needed

Short trip time → High $\frac{\text{Engine Power}}{\text{Spacecraft Mass}}$ (α)

Reduced IMLEO → High Exit Velocity (I_{sp})

Solution:

FDR Engine Specifications
Isp = 5000 s
Power Input= 180 kW
Gain 200
Power(Jet)= 36 MW
Spacecraft Mass = 15 MT
Payload Mass = 61 MT

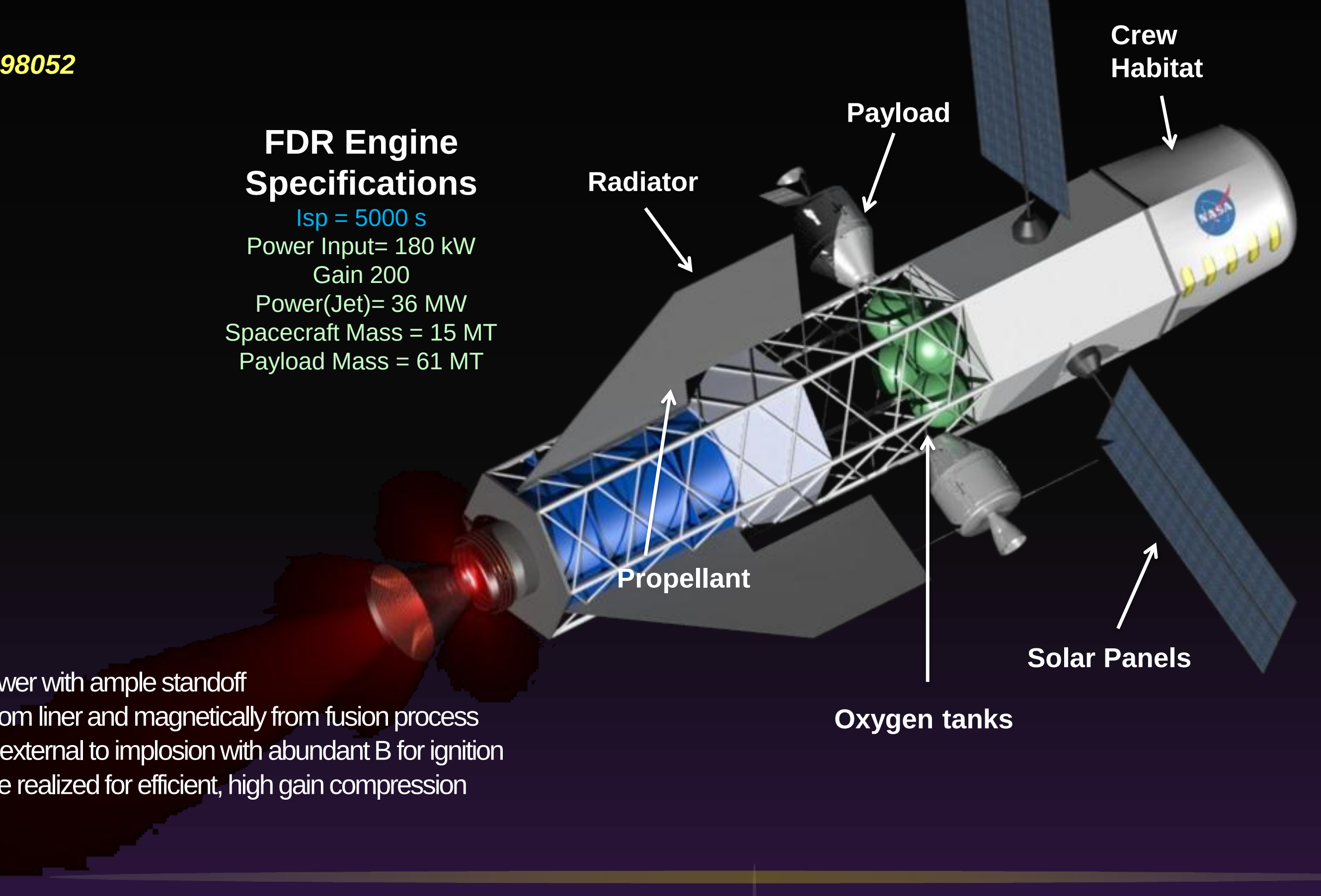

FDR Advantages:

- Large driver coil easy to power with ample standoff
- Driver electrically isolated from liner and magnetically from fusion process
- Large FRC can be formed external to implosion with abundant B for ignition
- Full 3D compression can be realized for efficient, high gain compression

Manned Mars Mission Architecture

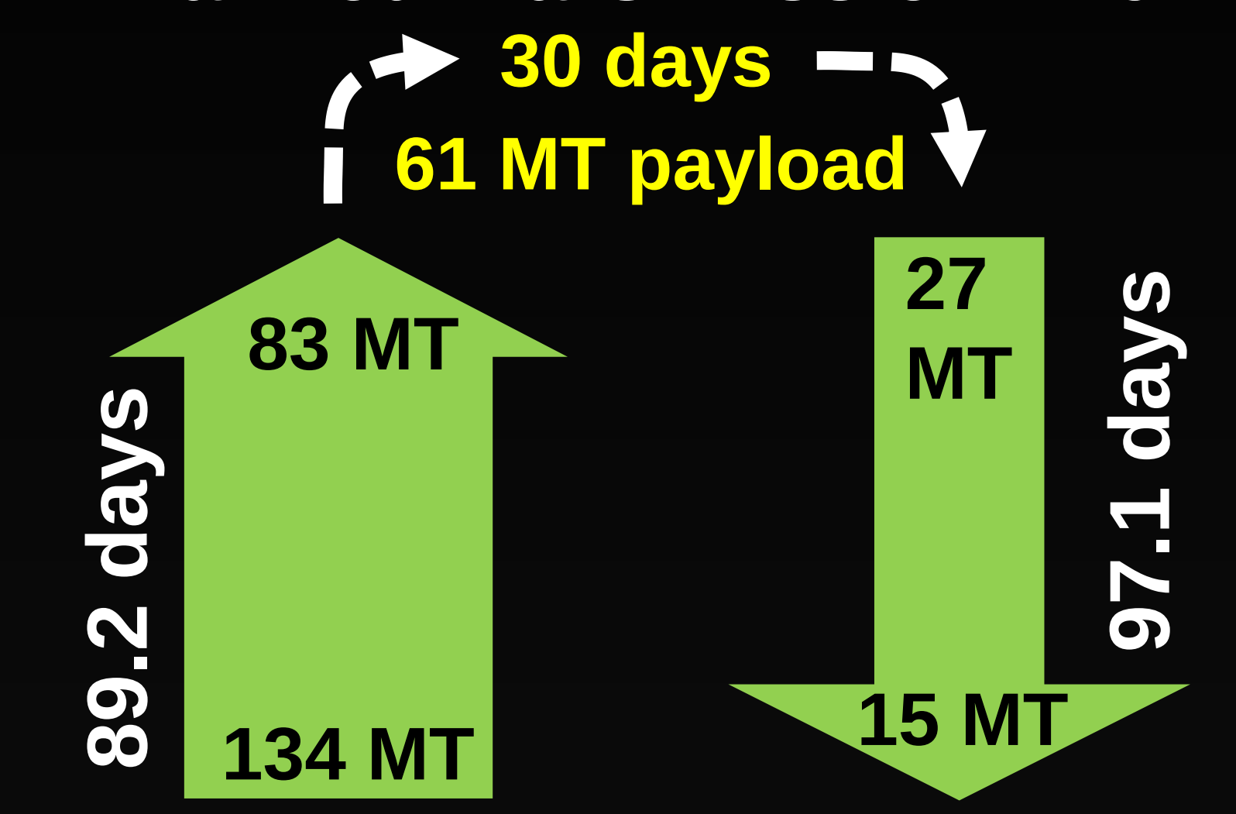

Mars mission based on nuclear thermal rocket
DRA 5.0 (NTP), 9 launches, 848.7 MT IMLEO, 1680 days

Mars mission based on Fusion driven rocket
DRA 5.0 (FDR), 1 launch, 134 MT IMLEO, 210 days

Approach/Design

Simplified animation illustrating the concept behind FDR

Concept Video

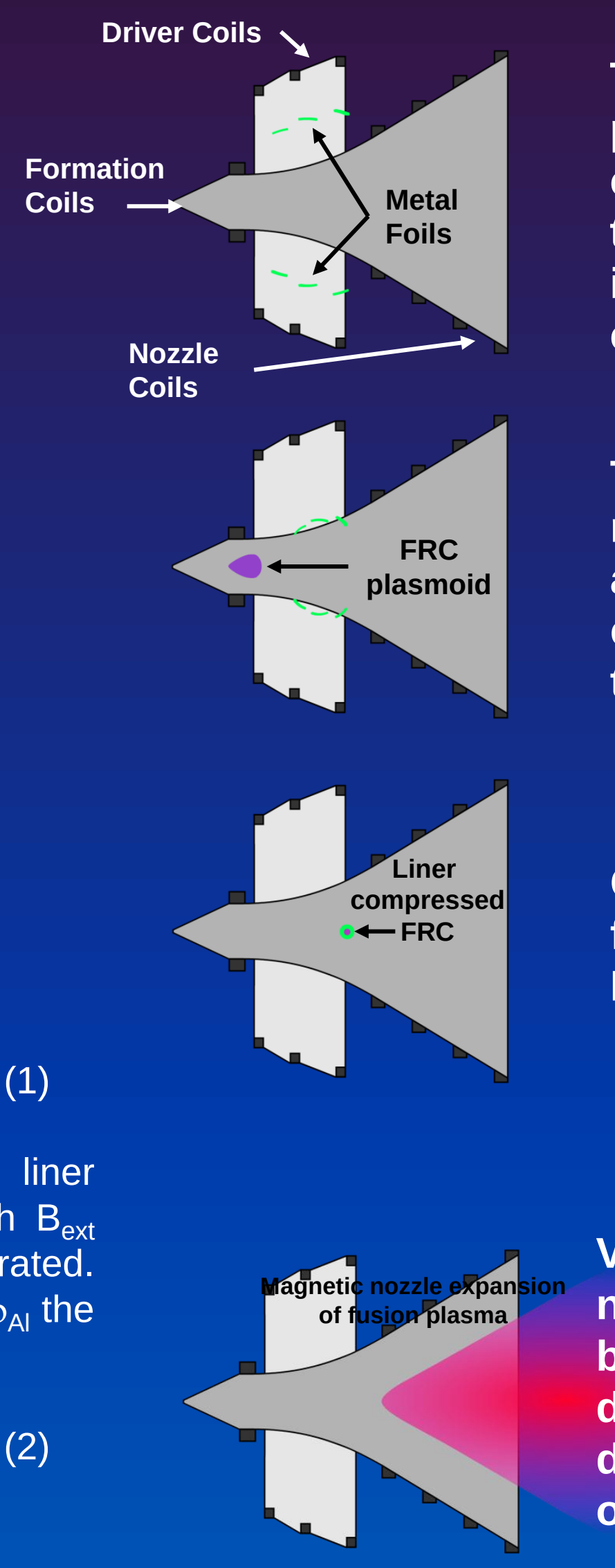

Thin hoops of metal are driven at the proper angle and speed for convergence onto target plasmoid at thruster throat. Target FRC plasmoid is created and injected into thruster chamber.

Target FRC is confined by axial magnetic field from shell driver coils as it translates through chamber eventually stagnating at the thruster throat

Converging shell segments form fusion blanket compressing target FRC plasmoid to fusion conditions.

Vaporized and ionized by fusion neutrons and alphas, the plasma blanket expands against the divergent magnetic field resulting directed flow of the metal plasma out of the magnetic nozzle.

Foil Liner Compression

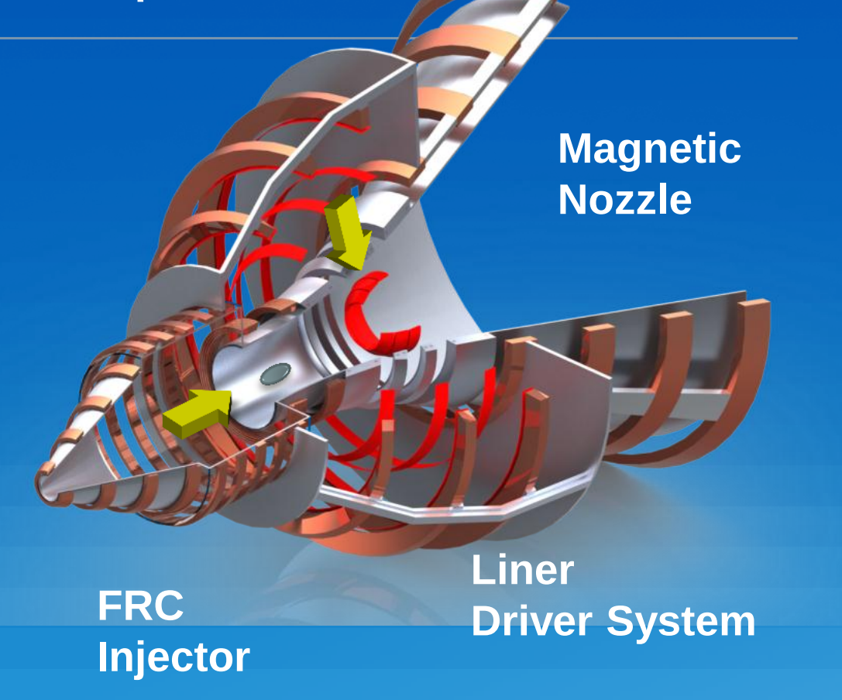

The dynamics of the liner implosion are governed by the equation:

$$M_L \frac{d^2 r}{dt^2} = \left(\frac{B_{in}^2}{2\mu_0} - \frac{B_{ext}^2}{2\mu_0} \right) 2\pi r w \qquad (1)$$

where M_L is the liner mass, and w the liner width. During the liner acceleration very little flux leaks through the liner ($B_{in} << B_{ext}$. With B_{ext} approximately constant during acceleration, Eq. (1) is readily integrated. With the liner mass $M_L = 2\pi r_L w \delta \rho_{Al}$ where δ is the liner thickness, and ρ_{Al} the density of Aluminum, the liner velocity is:

$$v_L = \left(\frac{r(t)}{2\mu_0 r_L \delta \rho_{Al}} \right) B_{ext}^2 t \quad = 125 \frac{\tau_{1/4}}{\delta} B_{ext}^2 \qquad (2)$$

The energy within the FRC separatrix at peak compression is dominated by plasma energy that is in pressure balance with the edge magnetic field B_0, so that one can write:

$$E_k = \frac{1}{2} M_L v_L^2 = 3 n_0 k T_0 \cdot \frac{4}{3} \pi r_0^3 \varepsilon = \frac{B_0^2}{\mu_0} \pi r_0^3 \varepsilon \qquad (3)$$

Where the zero subscript indicates values at peak compression. The last expression in Eq. (3) reflects the reasonable assumption that $r_s \sim r_0$ and magnetic pressure balance ($2n_0kT_0 = B_0^2/2\mu_0$). One has then for the energy gain from fusion produced in the FRC during the shell's dwell time at peak compression:

$$G = \frac{E_{fus}}{E_k} \quad = \quad 1.73\times10^{-3} \sqrt{\frac{M_L}{l_0}}\, B_0 \quad = \quad 4.3\times10^{-8} \sqrt{M_L}\, E_k^{11/8} \qquad (4)$$

where l_0 (= $2r_0 \cdot \varepsilon$) is the length of the FRC at peak compression. The last expression in Eq. (4) is obtained from adiabatic scaling laws for FRCs.

Experiment

ANSYS Video

ANSYS Multiphysics® calculation of the 3D behavior of three 40 cm radius, 5 cm wide, 0.2 mm thick Aluminum liners converging onto a stationary test target. The scale of the ellipsoid target (1×3.5 cm) is that anticipated for an initially 20 cm radius FRC compressed to 1 megabar energy density

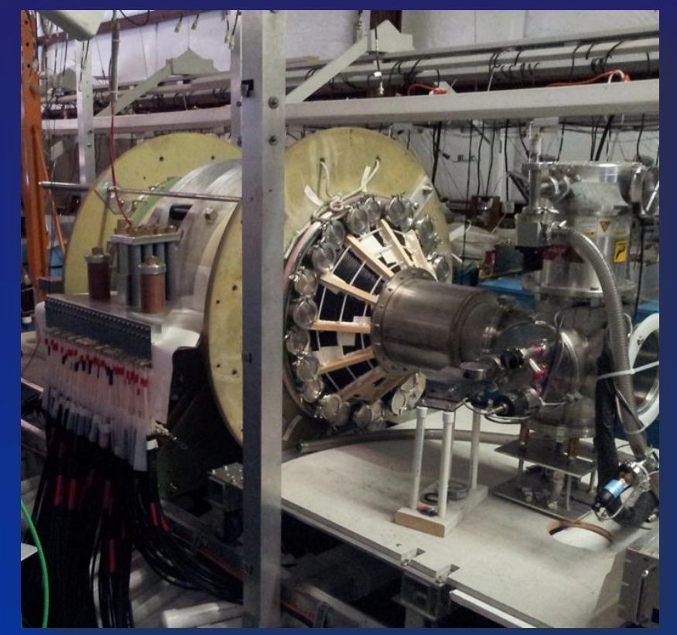

FDR validation experiment at the Plasma Dynamics Lab (UW)

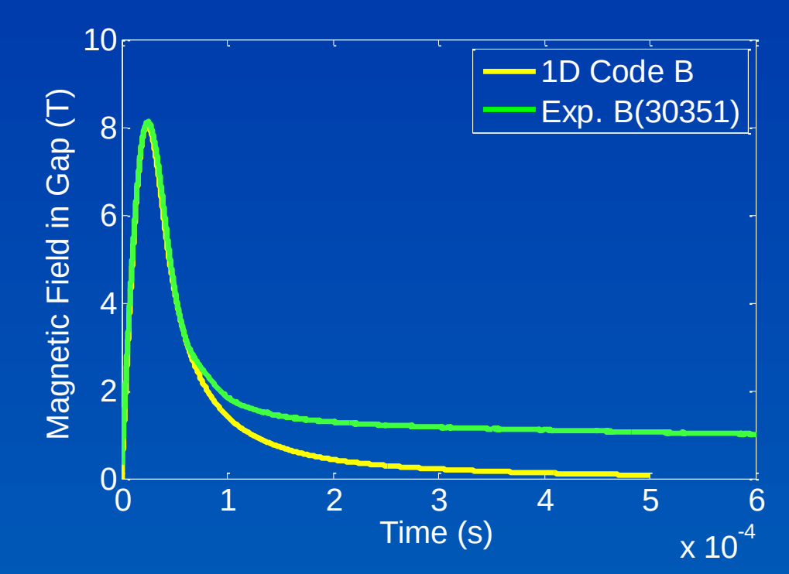

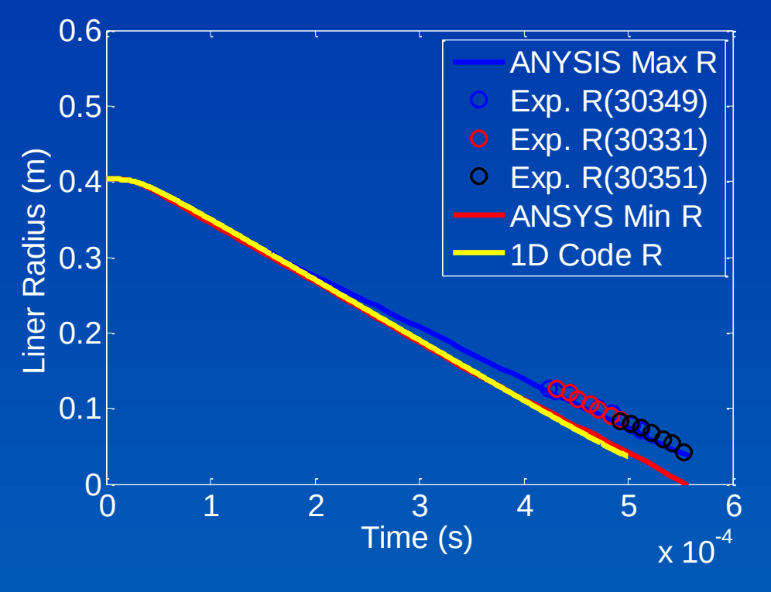

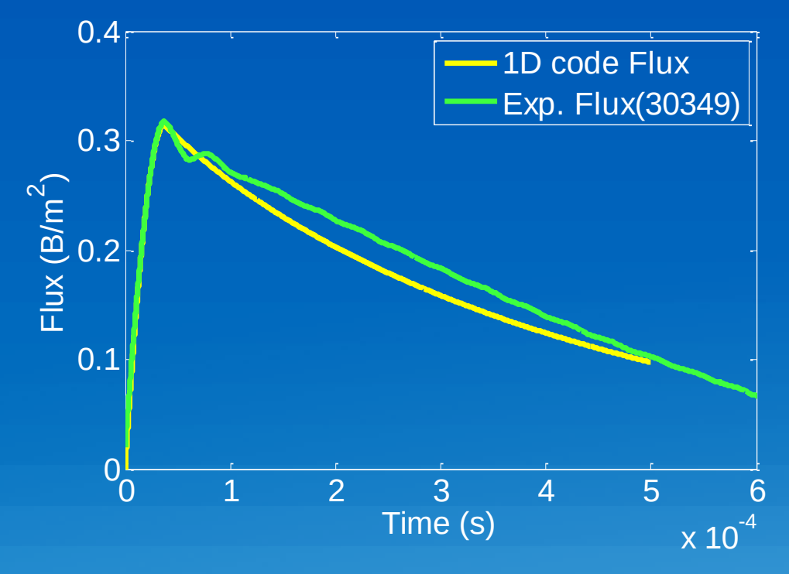

1D Liner Compression code calculation of the 40 cm radius, 6 cm wide, 0.4 mm thick Aluminum liners with a 840 μF, 20 kV driving circuit. Numerical model shows good agreement with experimental results for flux, B field, and position. Discrepancy in position is due to loss of energy in internal stress and strains of the liner. This effect is not captured in the 1D liner code, but is predicted accurately via ANSYS simulations.

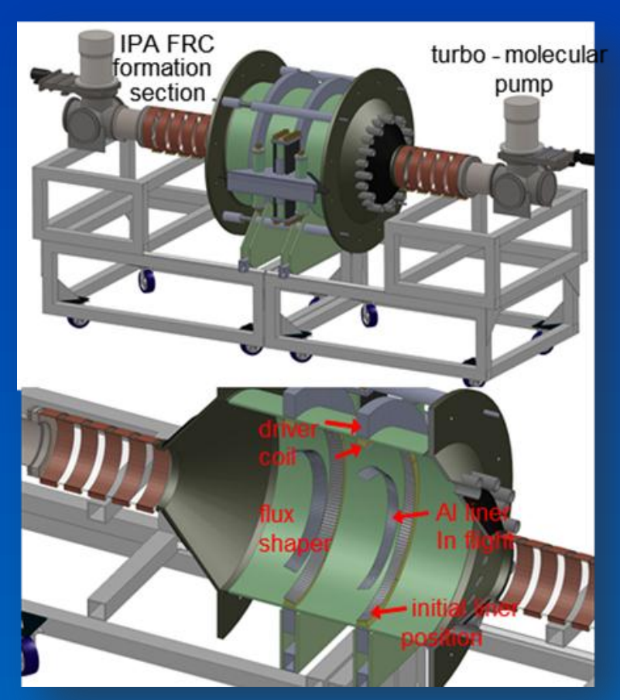

CAD rendering of the Foil Liner Compression (FLC) test facility at MSNW

¼ Power Aluminum Liner Testing for code Validation

20 kV | 840 μF |16 mil

Modeling

2D resistive MHD calculation of the formation and merging of FRCs inside the converging liners

MOQUI Video

Payload mass fraction 46%

Spacecraft Component	Mass (MT)	TRL	Mission Dependent	Fusion Dependent
Spacecraft structure	6.6	4	X	
Propellant tank	0.1	5	X	X
FRC Formation	0.2	4		X
Propellant Feed	1.2	2		X
Energy storage	1.8	7		X
Liner driver coils	0.3	3		X
Switches and cables	1.8	6		X
Solar Panels	2.7	8	X	X
Thermal Management	1.3	5		X
Nozzle	0.5	2		X
Spacecraft Mass	15		X	X
Crew habitat	61		X	
Propellant	57		X	X
Total Mass	133		X	X

1D Liner Code

Source Free RLC Circuit

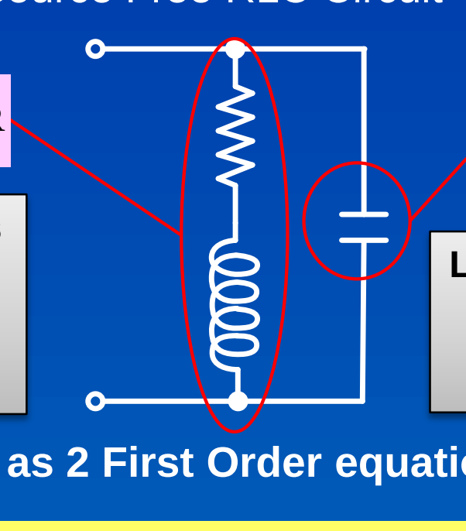

$$V = L\frac{dI}{dt} + I\frac{dL}{dt} + IR$$

$$I = C\frac{dV}{dt}$$

Circuit Parameters
R=3.5 mΩ
L=155 nH
840 uF
40,000 V

Liner Parameters
r=0.41 m
w=6 cm
l= 0.4 mm

Solved as 2 First Order equations

$$Yield = E_{fus} / E_{input} \cong \frac{1.2\times10^{-12}}{(2\mu_0 e)^2} B_0^4 r_l^2\, l_l\, \tau_D / E_{input}$$

Dwell time (70% of peak field)

Data for actual coil and collector plate used
In Foil Liner Compression
(FLC) Test bed

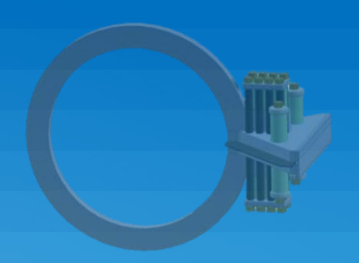

- **Various Current waveforms**
  - **Ringing**
  - **Crowbar**
  - **Diode**
- **Magnetic flux diffusion**
- **Resistivity - ρ(T)**
- **Latent heats**
- **Radiative cooling**
- **Energy conservation**

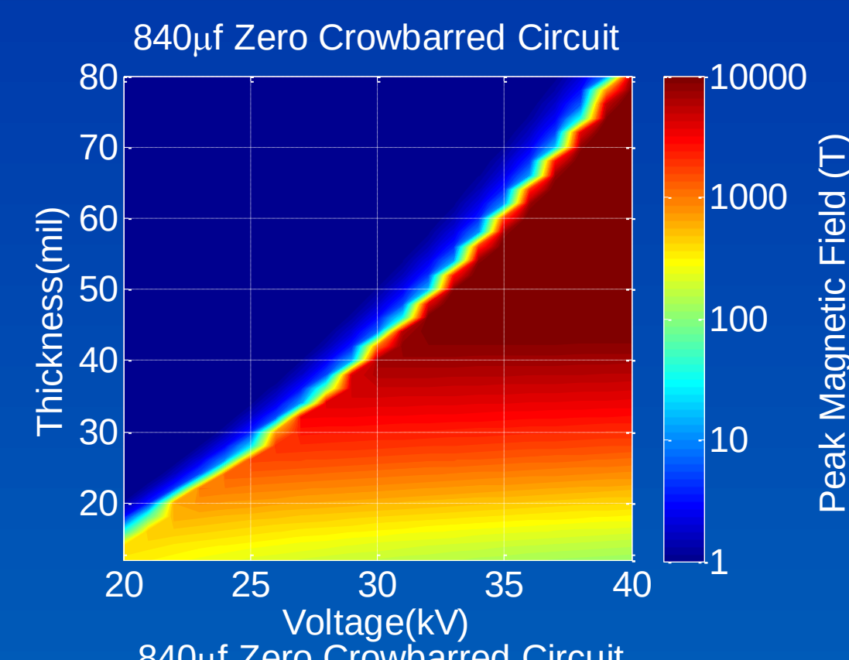

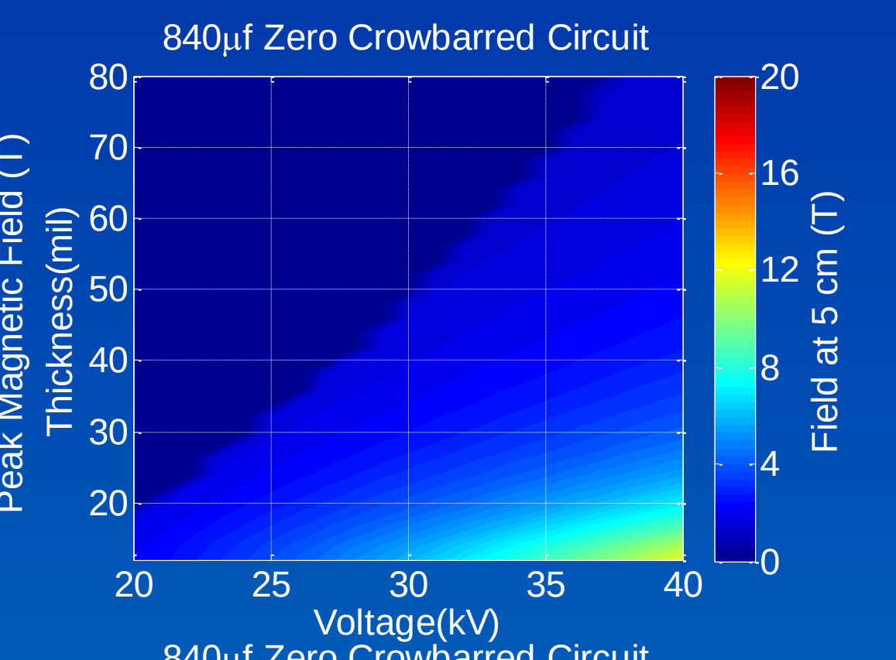

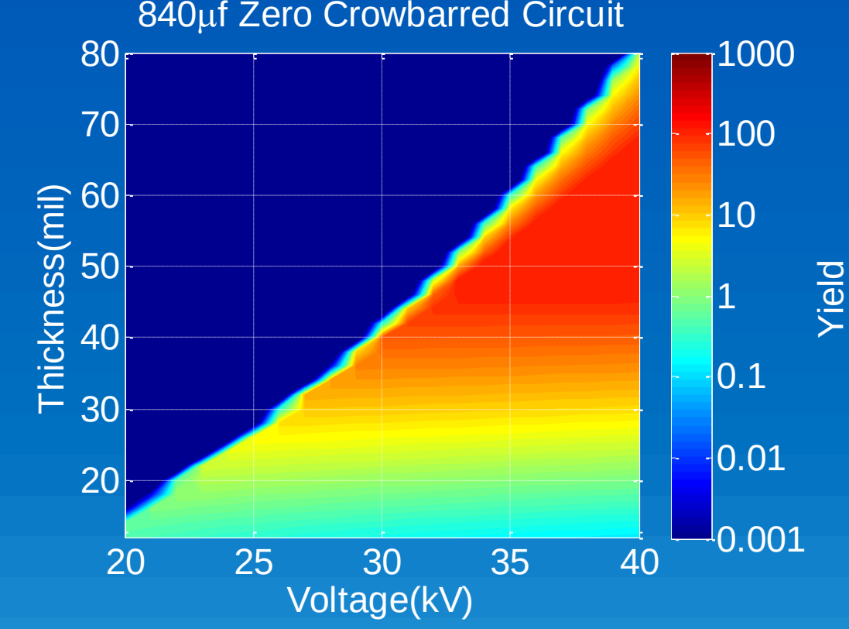

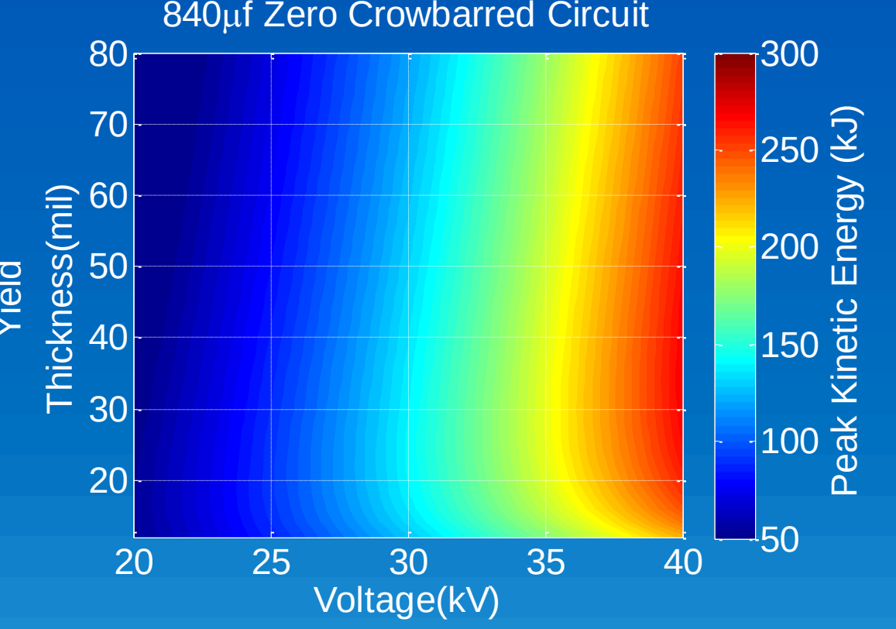

NIAC Spring Symposium

March 12-14, 2013

Chicago, Illinois